Time Evolution of Power Spectrum Density in Spontaneous Transition in Cylindrical Magnetized Plasma[*)]

Tatsuya KOBAYASHI[1)], Shigeru INAGAKI[2,3)], Stella OLDENBÜRGER[3)],
Katsuyuki KAWASHIMA[1)], Noriko OHYAMA[1)], Yuuki TOBIMATSU[1)], Hiroyuki ARAKAWA[4)],
Makoto SASAKI[2,3)], Yoshihiko NAGASHIMA[2,3)], Takuma YAMADA[3,5)], Satoru SUGITA[2)],
Masatoshi YAGI[2,3,4)], Naohiro KASUYA[3,6)], Akihide FUJISAWA[2,3)], Sanae-I. ITOH[2,3)] and
Kimitaka ITOH[1,3,6)]

[1)]*Interdisciplinary Graduate School of Engineering Sciences, Kyushu University, Fukuoka 816-8580, Japan*
[2)]*Research Institute for Applied Mechanics, Kyushu University, Fukuoka 816-8580, Japan*
[3)]*Itoh Research Center for Plasma Turbulence, Kyushu University, Fukuoka 816-8580, Japan*
[4)]*Japan Atomic Energy Agency, Naka, Ibaraki 311-0193, Japan*
[5)]*Graduate School of Frontier Sciences, The University of Tokyo, Tokyo 277-8561, Japan*
[6)]*National Institute for Fusion Science, Gifu 509-5292, Japan*

Preliminary observation results are reported for a new discharge regime in the Plasma Assembly for Nonlinear Turbulent Analysis (PANTA), where spontaneous transitions in the equilibrium profile and fluctuation spectra occur. Two different states are defined by using the mean density value. Axial and radial profiles are observed for the two states, and large profile changes are found. The spatiotemporal evolution of the transition front is measured. Changes in the fluctuation spectrum are evaluated using conditional average and lock-in average.

1. Introduction

Plasma turbulence can give rise to intermittent phenomena such as spontaneous structure formation or abrupt changes of the fluctuation regime [1]. Fast transitions between quasi-stable turbulent states like the L-H transition [2, 3] have been observed in fusion devices, but their theoretical understanding remains a challenge [4–6]. Understanding of such turbulent states and transitions is regarded as an important issue both in physics of non-equilibrium systems and in nuclear fusion research.

Transition phenomena have been successfully studied in several low temperature laboratory plasmas using multipoint measurements of plasma fluctuations [7–9]. In the PANTA, the successor device of the LMD-U, various turbulent regimes, some of which feature spontaneous transitions, can be investigated by changing the neutral gas pressure or the magnetic field strength. With a magnetic field strength of $B = 0.09$ T and high neutral gas pressure conditions ($P_n \sim 0.40$ Pa), a large amplitude coherent fluctuation accompanied by higher order harmonics, which is regarded as a drift solitary wave, is seen [10]. When the neutral gas pressure is lowered to an intermediate value ($P_n \sim 0.27$ Pa), the PANTA shows a transition region,

where the shape of the fluctuation spectrum switched spontaneously between two states [8, 9]. Finally, at low neutral gas pressure conditions ($P_n \sim 0.13$ Pa), a broad fluctuation spectrum is observed that had been associated with a streamer structure in the LMD-U [11, 12]. It has now been discovered, that a transition region can also be observed for a pressure between the intermediate and the low neutral gas pressure condition (at $P_n \sim 0.16$ Pa). In this regime, transitions are observed for the equilibrium profile as well as for the fluctuation spectrum. This article presents preliminary observations in the new transition regime.

2. Experimental Setup

Experimental observations are carried out in the PANTA, a linear cylindrical magnetized helicon plasma. The vacuum vessel of the PANTA has a length of 4050 mm and a diameter of 450 mm. Seventeen linearly aligned magnetic coils generate a homogeneous magnetic field with a fixed magnetic field strength of $B = 0.09$ T. Neutral (Argon) gas is fed in a glass tube installed at one side of the device and ionized by a 3 kW, 7 MHz RF source. Neutral gas pressure is monitored with two ion gauges at the source region and two manometers at the central region of the vacuum vessel, and can be controlled with a mass flow controller. The PANTA is equipped with several Langmuir probes to measure plasma fluctuations. The
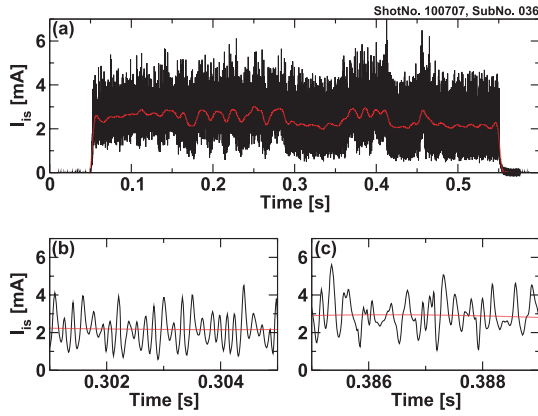
Fig. 1 (a) Typical time evolution of ion saturation current signal measured with one tip of the 64-channel probe array ($r = 4$ cm, $z = 1.625$ m, $\theta = 0$). Red curve shows 0.1 kHz cut-off low pass filtered signal. Two zoomed time series for the two different states are shown in (b) and (c).

Fig. 2 Normalized histogram of I_{is0}. The two fitting curves (red and green) are Gaussian fits for the two peaks. Labels show mean value and standard deviation of the fitted Gaussians.

measurement location of each probe tip is given in cylindrical coordinates, r, θ and z, where the origin of the z coordinate is defined as the plasma helicon source. In this article, we use three kinds of probe sets: a 64-channel azimuthal probe array ($r = 4$ cm, $z = 1.875$ m, $-\pi < \theta < \pi$), a 5-channel radial probe array ($2 < r < 6$ cm, $z = 1.625$ m, $\theta = \pi$), and a 4-point axially aligned probe set ($r = 4$ cm, $z = 1.125, 1.625, 1.875$ and 2.625 m, $\theta = 0$) to observe the three-dimensional evolution of the transition front and fluctuation. We use one tip of the 64-channel azimuthal probe array at $\theta = 0$ as a reference to detect the onset of the transition. The ion saturation current fluctuations are measured with a temporal resolution of $\Delta t = 1$ μs, and can be used as an index of the electron density fluctuations [13].

3. Experimental Results
3.1 Identification of the transition
Figure 1 shows the typical time evolution of the ion saturation current signal measured with the reference probe. The red dashed curve shows the low pass filtered signal using a cut-off frequency $f_c = 0.1$ kHz. The low pass filtered signal I_{is0} follows the mean density evolution during the discharge. It is easy to see that I_{is0} transits between a lower and higher value. Time series for each state can be selected manually and examples are given in Fig. 1 (b) for the lower mean density and Fig. 1 (c) for the higher mean density. Qualitative differences in the fluctuations' shape are seen. To discuss the changes in I_{is0} more quantitatively and detect transitions automatically, we first inspect the normalized histogram of the I_{is0} value which is given in Fig. 2 for 50 discharges. Two separate peaks appear in the normalized histogram and are the sign of a bifurcation in I_{is0} between two different states. We assume the probability density of I_{is0} for each state has the shape of a Gaussian distribution. The nonlinear least squares Gaussian fitting for each peak are shown by red and green curves in Fig. 2,
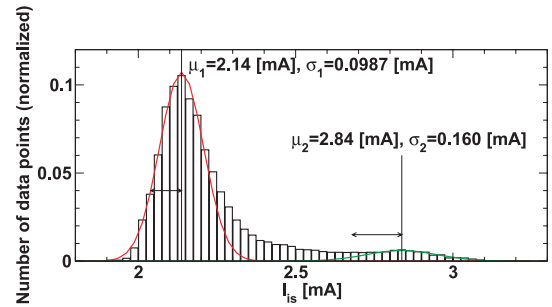
where the mean values and standard deviations for each Gaussian are indicated in the labels. Using these Gaussian parameters, we can explicitly define two states, called the lower and upper state, as $|I_{is0} - \mu_1| \leq \sigma_1$ and $|I_{is0} - \mu_2| \leq \sigma_2$, respectively. Because the area in the normalized histogram for the lower state is much larger than the one for the upper state, the plasma is predominantly in the lower state, and sometimes abruptly transits to the upper state. We define the transition onset time as the moment in time when the I_{is0} signal rises to the threshold value $\mu_2 - \sigma_2$ (we call a fall below the threshold value an inverse transition).

3.2 Changes in the equilibrium profiles
Figures 3 (a) and (b) show axial and radial profiles for the two states calculated with conditional averaging. Typical transition time is a few milliseconds. In the axial profile, values of averaged I_{is} decay as the axial position z increases in both states, presumably due to plasma recombination loss. However, characteristic I_{is} fluctuations at different axial positions are qualitatively similar and their cross coherences are quite high for specific modes. We may therefore regard the plasma turbulence as two-dimensional even if a density gradient exists in the axial direction. Differences in I_{is0} profiles are seen in both the axial and radial direction for the two states. In the plasma core region, at $r = 2$ cm, I_{is} changes by 30-40%.

We estimate the spatiotemporal evolution of equilibrium profiles transition in both axial and radial direction using the low pass filtered signals. Cross Correlation Function (C.C.F) is calculated between the signals at two different axial (radial) positions for over 90 transitions and inverse transitions, and we obtain time lags τ with quite high C.C.F values. Figure 4 is a plot of the time lag τ as a function of measurement location. In the axial direction, shown in Fig. 4 (a), the time lag is computed by using the probe tip at $z = 1.125$ m, closest to the source region as a reference. Positive τ, indicating time delay, is observed. The value $dz/d\tau$ indicates propagation speed of the transition front and seems to decrease as the measurement point moves away from the source region. The time
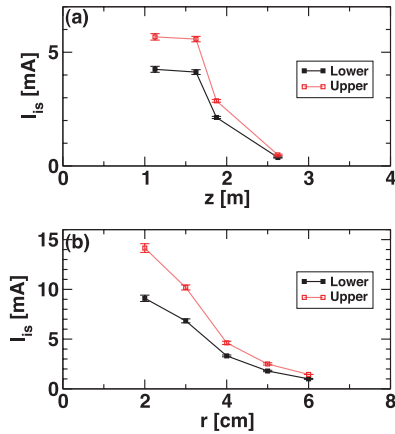
Fig. 3 Conditional averaged (a) axial and (b) radial profiles for the upper and lower states. Error bars show the standard deviation from over 90 distinct transitions in 50 shots.
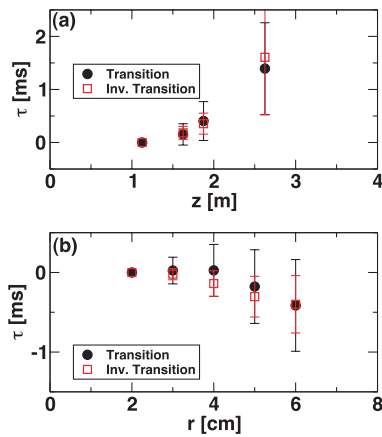
Fig. 4 Time lags of transition and inverse transition onsets in the (a) axial and (b) radial direction, calculated with reference probes at $z = 1.125$ m and $r = 2$ cm, respectively.

delay for the plasma near the source region $z < 1.125$ m is quite small, showing that the transition occurs simultaneously in this region. Roughly estimated propagation speed at $z \sim 1 - 2$ m is slightly less than ~ 2000 m/s, which is of the order of the ion sound speed $C_s \sim 2000$ m/s. Far from the source region, at $z > 2$ m, a decrease in the electron temperature is expected, resulting in a decrease of C_s. This could be linked with the observed propagation speed decay, but more data is necessary to confirm this observation, as error bars are too large in Fig. 4 to conclude unambiguously. In the radial direction, the value τ is calculated with respect to a reference at $r = 2$ cm and is shown in Fig. 4 (b). Negative τ decreasing with increasing r is observed. The transition seems to first occur at the edge region and to develop towards the core region with a characteristic speed of ~ 60 m/s. Again, time lag in the core region of $r < 2$ cm is quite small. In general, the propagation speed can be quite different for each transition event, resulting in large error bars that make statistical quantitative evaluation difficult.

Nevertheless, the qualitative features of the transition are comparable for most of the transition events.

3.3 Changes in the fluctuations

As seen in Figs. 1 (b) and (c), the fluctuation waveform also changes as the transition takes place. In this subsection, we study the features of the fluctuation spectra for the two states and during the transition. Azimuthal propagation of the ion saturation current fluctuations is observed with every other tip of the 64-channel probe array. We define the positive direction for the azimuthal angle θ as the direction of electron diamagnetic drift. Windowed Fourier Transform (FT) is performed for both time and azimuthal space to calculate the two-dimensional power spectral density as a function of frequency f and azimuthal mode number m, where the sign of the mode number gives the propagation direction. A time window of $\Delta T = 3$ ms is used to obtain a frequency resolution of $\Delta f = 0.3$ kHz. Figures 5 (a) and (b) are conditional averaged power spectral density for the lower and upper states. In the lower state, the dominant fluctuating mode is located at $(m, f) = (2, 6.7 \text{ kHz})$. In addition, a counter-propagating mode at $(m, f) = (-1, 1.3 \text{ kHz})$ is excited. In the upper state, the counter-propagating mode is still observed but its frequency slightly changes to $f = 1.0$ kHz. The mode number and frequency of the dominant mode are changed to $(m, f) = (1, 2.3 \text{ kHz})$. The broad spectra can have many combinations of three-wave coupling. In particular, three-wave couplings involving the counter-propagating mode have been considered playing an important role for the nonlinear excitation process of the streamer structure in the LMD-U [12]. We discuss similarities between the spectra for the two states and the spectra obtained for discharges with slightly decreased and increased neutral gas pressure. In both neighboring neutral gas pressure conditions, no transitions are observed, and fluctuation spectra remain unchanged during the whole discharged. Fluctuation spectra for the cases of $P_n = 0.13$ Pa and $P_n = 0.17$ Pa are drawn in Figs. 5 (c) and (d). To see differences in the spectra more quantitatively, mode number integrated power spectrum densities for Figs. 5 (a) and (b), and Figs. 5 (c) and (d) are shown in Figs. 5 (e) and (f), respectively. The fluctuation spectrum in the lower state is similar to the one in the $P_n = 0.13$ Pa case, and the spectrum in the upper state resembles the one in the $P_n = 0.17$ Pa case. Assuming that the two pairs of similar spectra indicate same fluctuation states, there might be possible multiple fluctuation states at this regime.

In the last part of the present article, we observe the time evolution of fluctuating mode power during the transition and inverse transition using the lock-in average technique. The lock-in average at the moment of the transition and inverse transition is defined as $\bar{x}(\tau) = 1/N \sum_{i=1}^{N} x(t_i + \tau)$, where $\tau = -M\Delta t/2, -(M-1)\Delta t/2, \ldots, 0, \ldots, (M-1)\Delta t/2$ and $M\Delta t$ is a specific time width. The value t_i
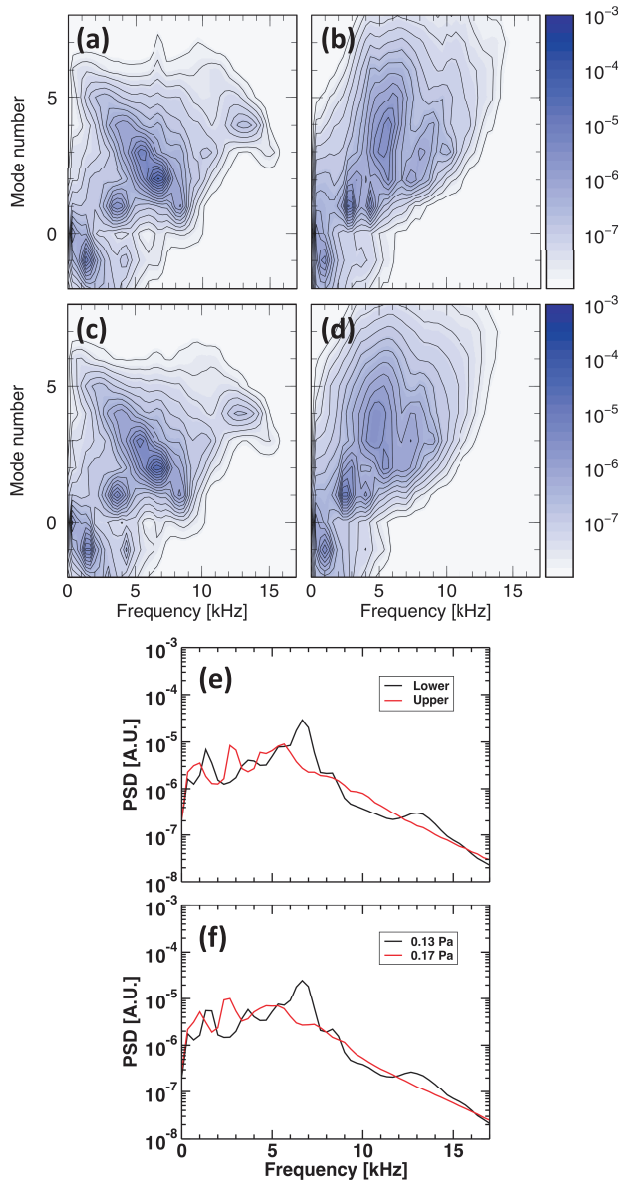
Fig. 5   Conditional averaged two-dimensional power spectral density for (a) the lower state and (b) the upper state. For comparison, the spectra for discharges in the (c) $P_n = 0.13$ Pa case and (d) $P_n = 0.17$ Pa case are shown. Mode number integrated power spectrum density of (a) and (b) is shown in (e) and that of (c) and (d) is shown in (f).

indicates the i-th transition (or inverse transition) and N is the total number of transitions (or inverse transitions). It should be noted that this lock-in average is generally called conditional average and is widely used (e.g., to observe shapes of plasma blobs [14]). Here, we focus on two characteristic modes in the lower state, i.e., the modes at $(m, f) = (2, 6.7\,\text{kHz})$ and $(m, f) = (-1, 1.3\,\text{kHz})$. The time window of the FT is shifted by steps of 0.05 ms to obtain the time evolution of the spectrum. The power spectral density of the $m = 2$ mode is integrated over a frequency range corresponding to the half-width of the mode. For the counter-propagating mode, we use the integration
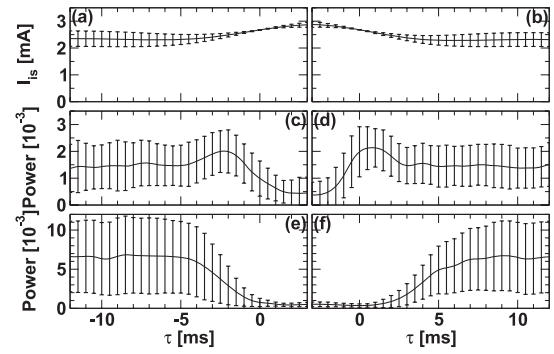
Fig. 6   Time evolution of (a) and (b) I_{is0} signal, (c) and (d) fluctuating mode powers of the counter-propagating mode, and (e) and (f) those of the $m = 2$ mode, calculated using lock-in average for transitions and inverse transitions.

range $0\,\text{kHz} \leq f \leq 3.0\,\text{kHz}$ to account for the slight frequency change during the transition. Figures 6 (a), (c) and (e) show the lock-in averaged time series of I_{is0} and fluctuation powers for the counter-propagating mode and the $m = 2$ mode, around the moment of the transition. Figures 6 (b), (d) and (f) are the corresponding plots for the inverse transition. The error bars represent standard deviation. One can compare the time series of the mode power variation with that of I_{is0}. For the transition case, first the power of the counter-propagating mode starts to increase, that of the $m = 2$ mode starts to decrease and the I_{is0} starts to increase. After a few millisecond, the evolution of the counter-propagating mode changes and its power starts to decrease. For the inverse transition, growth of the counter-propagating mode power and accompanying decrease of I_{is0} is seen before the growth of the $m = 2$ mode power. Moments with strong $m = 2$ mode power seem to be related to a damping of the counter-propagating mode power in both cases. This may imply that an energy interchange exists between these two modes. As shown in Fig. 6, the causal relation between fluctuation power variation and I_{is0} variation is not easy to clarify. Indeed, an interactive connection exists between fluctuations and mean density. Changes in fluctuations can vary the profile through changes in transport, and changes in the profile can also affect fluctuations by changing the growth rate of the fluctuations. To draw a conclusion, further measurements are needed to study the dynamics of the transport and gradients.

4. Summary

Experimental observations of a new abrupt transition phenomenon in both the equilibrium profiles and the fluctuation spectra were reported. The mean component of the ion saturation current signal, calculated with a 0.1 kHz cutoff low pass filter, was used to identify two different states called the upper and the lower state. A normalized histogram of the mean value of ion saturation current showed

a distribution with two peaks and was fitted with two Gaussians. Two states were explicitly defined by using parameters from these two Gaussians and transition detection could be automated. Changes in the equilibrium profile were observed with mean values of ion saturation current changed by 30-40% in the plasma core region. Spatiotemporal evolution of the profile transition front was measured. In the axial direction, the transition seemed to occur simultaneously in the first quarter of the plasma near the source region, and to evolve towards the end plate. A characteristic speed close to C_s was estimated in the middle of the plasma column. In the radial direction, the transition seemed to start close to the edge of the plasma and to develop towards the core region at a speed of ~ 60 m/s.

Two-dimensional Fourier power spectral density was calculated as a function of frequency and azimuthal mode number. Conditional averaged power spectra in the two different states were found to be similar to the averaged power spectra at both neighboring neutral gas pressure conditions, implying that there might be multiple fluctuation states for the transition conditions. In the last part of this article, we showed lock-in averaged time sequences of fluctuating power for several characteristic modes during the transition and inverse transition. Possible evidence could be presented that energy was exchanged between several modes.

[1] K. Itoh *et al.*, *Transport and structural formation in plasmas* (Institute of Physics Pub., 1999).
[2] F. Wagner *et al.*, Phys. Rev. Lett. **49**, 1408 (1982).
[3] M. Nagami *et al.*, Nucl. Fusion **24**, 183 (1984).
[4] S.-I. Itoh *et al.*, Phys. Rev. Lett. **60**, 2276 (1988).
[5] P. Diamond *et al.*, Phys. Rev. Lett. **72**, 2565 (1994).
[6] J. Cordey *et al.*, Nucl. Fusion **35**, 101 (1995).
[7] Y. Nagashima *et al.*, J. Plasma Fusion Res. SERIES **8**, 50 (2009).
[8] H. Arakawa *et al.*, Plasma Phys. Control. Fusion **51**, 85001 (2009).
[9] H. Arakawa *et al.*, Plasma Phys. Control. Fusion **52**, 105009 (2010).
[10] H. Arakawa *et al.*, Plasma Phys. Control. Fusion **53**, 115009 (2011).
[11] T. Yamada *et al.*, Nat. Phys. **4**, 721 (2008).
[12] T. Yamada *et al.*, Phys. Rev. Lett. **105**, 225002 (2010).
[13] K. Kawashima *et al.*, Plasma Fusion Res. **6**, 2406118 (2011).
[14] T. Carter, Phys. Plasmas **13**, 010701 (2006).